AAPT PHYSICS EDUCATION | AMERICAN JOURNAL of PHYSICS

Fourier analysis of thermal diffusive waves

Muhammad Sabieh Anwar, Junaid Alam, Muhammad Wasif, Rafi Ullah, Sohaib Shamim, and Wasif Zia

Citation: American Journal of Physics **82**, 928 (2014); doi: 10.1119/1.4881608
View online: http://dx.doi.org/10.1119/1.4881608
View Table of Contents: http://scitation.aip.org/content/aapt/journal/ajp/82/10?ver=pdfcov
Published by the American Association of Physics Teachers

Fourier analysis of thermal diffusive waves

Muhammad Sabieh Anwar,[a] Junaid Alam, Muhammad Wasif, Rafi Ullah, Sohaib Shamim, and Wasif Zia
Department of Physics, Syed Babar Ali School of Science and Engineering, Lahore University of Management Sciences (LUMS), Opposite Sector U, D. H. A., Lahore 54792, Pakistan

(Received 18 December 2012; accepted 22 May 2014)

We present details of an experiment that improves earlier attempts to study the propagation of diffusive thermal waves inside a metal rod. In addition to technical improvements in data acquisition and heater control, the experiment physically illustrates insightful concepts in Fourier analysis. For example, the harmonic content and the differential damping of harmonics can be observed in the thermal domain, thus providing a valuable extension to the standard Fourier analysis of electric circuits.
[http://dx.doi.org/10.1119/1.4881608]

I. INTRODUCTION

If a metallic sample is periodically heated at one end, thermal oscillations will propagate along the sample. This is the mainstay of a beautiful experiment performed by Bodas and co-workers,[1] where an application of the one-dimensional heat equation to a propagating thermal disturbance leads to the estimation of the thermal diffusivity of copper. In that paper, it is claimed that various Fourier components of the advancing disturbance are differentially damped; however, this claim was not experimentally observable as readings were manually read from a hand-held device while time was measured using a stopwatch. Here we show that by introducing computer-based control and data acquisition this experiment can be transformed into an elegant demonstration of Fourier analysis, enabling the harmonic content of a propagating disturbance to be visualized with astounding clarity. The key is inputting the data to a computer to allow for numerical operations, such as Fast Fourier Transformation (FFT) and the measurement of spectral density. The experiment therefore manifests as a beautiful demonstration of a *mathematical phenomenon*, to borrow Berry's expression,[2] something our students thoroughly enjoy.

It is interesting to understand the nature of these wave-like oscillations and to decipher whether they constitute a "wave" or not. The concept of a wave itself is not as simple as it seems,[3] although there are physical attributes that help us infer whether a particular phenomenon qualifies as a wave. First, these wave-like thermal oscillations do not transport energy.[4] Furthermore, they have no wavefronts, do not reflect or refract when encountering an interface, and cannot be transmitted in a preferred direction in a homogeneous medium.[5] Thus, these wavy thermal oscillations can by no means be regarded as waves similar to those that transmit sound or radio signals. Nevertheless, these oscillations are sometimes referred to in the literature as diffusion-waves, mainly because the accompanying transmission of energy or particles is diffusion limited.[5,6]

Being fundamentally different from conventional waves and having various important applications in different disciplines of science, diffusion-waves certainly deserve some attention. An in-depth investigation of the phenomena should help us understand the basic difference between conventional waves and diffusion-waves. Moreover, these diffusive thermal oscillations can be used in an undergraduate-level experiment[1] to measure the thermal properties of a material with high efficiency and reasonable accuracy. Although applications of diffusion-waves are not an immediate concern of this article, it is worth mentioning a few examples. When a modulated laser beam is irradiated on a surface, thermal diffusion waves are generated that in turn create a refractive index gradient. A probe laser moving parallel to the surface will then be deflected harmonically, a phenomenon known as the "mirage effect" that gives rise to a technique called Photothermal Deflection Spectroscopy (PDS). Another example is using intermittent laser heating and thermal expansion to create a thermoelastic deformation bump. Blackbody radiation can then be intercepted from the thermally oscillating surface in a technique called Photo-Thermal Radiometry (PTR). Lastly, a thermal oscillation can be generated inside a medium with a characteristic skin depth; the diffusing oscillation can be detected using a pyroelectric sensor in a technique known as Photo-Pyro-Electric Spectroscopy (PPES).[6]

II. THE EXPERIMENT

A. Apparatus

Our experiment is a modern adaptation of the original experiment by Bodas *et al.*[1] We use a 50-cm cylindrical copper bar with a homemade 25 -W cartridge heater inserted into one end. The rod is wrapped inside 4–5 turns of 1/8-in. fiberglass insulation paper to minimize heat loss. Figure 1 shows the experimental arrangement. A pulsed dc voltage set at 25 V supplies an intermittent current of 1 A to the heater and is switched into the circuit by means of an electromechanical relay actuated by a computer-generated signal. The heater is actuated at a frequency of $\omega_1/(2\pi) = 5$ mHz, applying a square-wave heating pulse to the bar. Temperatures at four different points along the bar are measured using K-type thermocouples whose cold-junction temperatures are monitored by a thermistor. The actuation pulse and temperatures are interfaced using National Instrument's PCI 6221 data-acquisition card. Adding computer interfacing provides unique insight into the physics of the problem because we can (a) accurately measure the oscillation amplitudes at multiple positions simultaneously as a function of time and (b) perform a Fast Fourier Transform (FFT) on the finely sampled numerical data sets.

B. Observations

The temperature variation for the four thermocouples, each separated by 3.3 ± 0.2 cm, is shown in Fig. 2 and

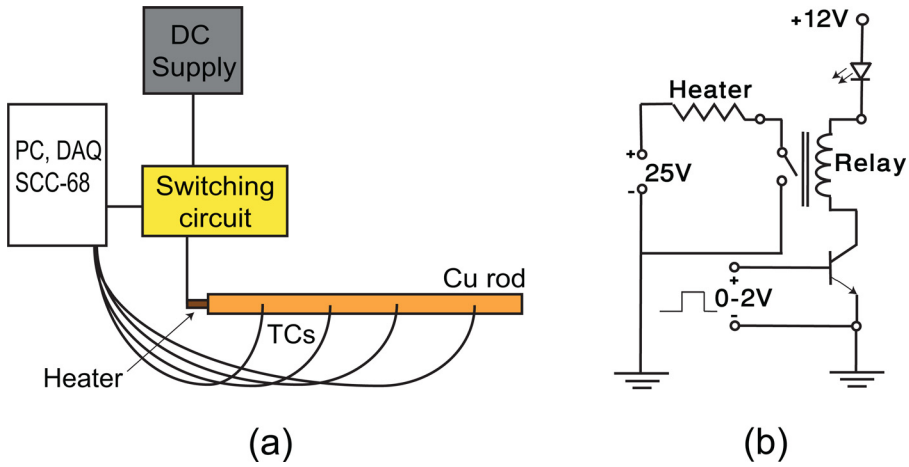

Fig. 1. (a) Schematic diagram of the experimental arrangement; (b) the switching circuit for actuating the heat source.

displays several noteworthy features. First, the temperatures vary in an oscillatory fashion riding on top of their respective average values. The average temperature rises in the transient stage and in about half an hour reaches a constant steady state; the oscillations persist until the heater is turned off. The thermocouple nearest the heat source registers an approximately triangular variation and the temperature becomes increasingly more sinusoidal as you move farther from the heat source. This (approximate) triangular shape arises out of a fortuitous choice of the actuation frequency and the distance of the first thermocouple from the heater's surface. We revisit the shape of this wave in Sec. II D. Eventually, at the thermocouple farthest from the heat source, the temperature fluctuation (now much smaller in amplitude) is nearly a perfect sinusoid. Second, we also observe that the oscillations are not in phase; there is a phase lag between successive thermocouples. Third, the average temperature for each thermocouple is different indicating the existence of a mean temperature gradient. It is only the gradient in the mean temperature field that in fact causes heat to transfer from the hot to cold end.[4] Last, we observe that all four thermocouples begin at the same temperature and, after the heater is turned off, the curves merge again showing equilibration of temperature and cessation of heat flow. In addition, the cooling region of the graph also provides a measure of the quality of insulation of the copper rod from its environment. In fact, one can fit the cooling data to an exponential function and determine the rate of convective heat transfer. Several laboratory experiments investigating radiative and convective heat transfer can be found in the literature.[8–10]

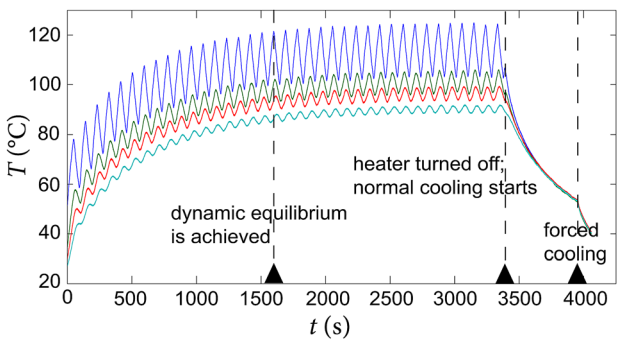

Fig. 2. Temperature oscillations at different points along the copper bar. The thermocouples closer to the heat source have higher average temperatures. A dynamic equilibrium is reached after about 30 min. At around 55 min the heater is switched off permanently and the assembly is allowed to cool, first under ambient conditions and then in the presence of a cooling fan.

C. Analysis

The mathematically rich structure of these fluctuations is analyzed using Fourier analysis. The diffusive nature of the oscillations is described by the one-dimensional heat equation

$$\frac{\partial^2 T}{\partial x^2} = \frac{1}{D}\frac{\partial T}{\partial t}, \tag{1}$$

where $T(x, t)$ is the temperature distribution along the rod, D is the (constant) thermal diffusivity, and $x = 0$ is taken to be the location of the first thermocouple. The solutions to the heat equation are extensively described in numerous textbooks and analytic solutions exist for special cases.[7,11] The special case relevant to our problem is one-dimensional heat conduction through a semi-infinite solid with temporally periodic boundary conditions. Given the periodic nature of the heating function, we seek a steady-state solution in the form of a Fourier series:

$$\begin{aligned} T(x,t) &= c_0(x) + \sum_{n=1,2,\ldots}^{\infty} c_n(x)\cos(\omega_n t - \varepsilon_n) \\ &= c_0(x) + \sum_{n=1,2,\ldots}^{\infty} c_n(x)\,\mathcal{R}\{e^{i(\omega_n t-\varepsilon_n)}\}, \end{aligned} \tag{2}$$

where the symbol $\mathcal{R}\{\cdots\}$ represents the real part of the function. Here, the c_n's are the (position dependent) Fourier coefficients, $\omega_n = n\omega_1$ are the Fourier frequencies, and ε_n are phase factors. Note that the position dependence is contained entirely in the Fourier coefficients and is separate from the time-dependent exponentials. The zero-frequency term $c_0(x)$ represents the mean temperature; in a moment we will explore whether such a bias term is admitted by Eq. (1). For notational convenience, we will drop the symbol $\mathcal{R}\{\cdots\}$ and remember to take the real part when appropriate.

Inserting the ansatz (2) into Eq. (1), we obtain

$$\frac{d^2c_0(x)}{dx^2}+\sum_{n=1,2,\ldots}^{\infty}\frac{d^2c_n(x)}{dx^2}e^{i(\omega_n t-\varepsilon_n)} = \sum_{n=1,2,\ldots}^{\infty} i\frac{n\omega_1}{D}\,c_n(x)e^{i(\omega_n t-\varepsilon_n)}, \tag{3}$$

and equating terms with the same time dependence leads to

$$\frac{d^2c_0(x)}{dx^2}=0 \quad \text{and} \quad \frac{d^2c_n(x)}{dx^2}=i\frac{n\omega_1}{D}\,c_n(x). \tag{4}$$

These equations can be solved to give

$$c_0(x)=P_1x+P_0 \tag{5}$$

$$c_n(x)=A_n\exp\left[(1+i)\sqrt{\frac{n\omega_1}{2D}}x\right] + B_n\exp\left[-(1+i)\sqrt{\frac{n\omega_1}{2D}}x\right], \tag{6}$$

where P_0, P_1, A_n, and B_n are constants that will be determined from appropriate boundary conditions. We note immediately that the bias term $c_0(x)$ has a linear position dependence, as expected. Furthermore, since we require finite temperatures as $x\to\infty$, we must have $A_n=0$ for all n. Hence, a possible solution to the heat-equation for our one-dimensional problem is

$$T(x,t)=(P_1x+P_0)+\sum_{n=1,2,\ldots}^{\infty}B_n\exp\left(-\sqrt{\frac{n\omega_1}{2D}}x\right) \times\exp\left[i\left(n\omega_1t-\sqrt{\frac{n\omega_1}{2D}}x-\varepsilon_n\right)\right]. \tag{7}$$

As mentioned, the constants are determined from the boundary conditions, which are, interestingly, measured and extracted from the experiment itself. As shown below, all of the constants except P_1 can be determined from the temperature oscillation at the location of the first thermocouple ($x=0$). Later, we can find P_1 by measuring the average temperature at any other location within the domain of experimental observation.

At $x=0$, Eq. (7) takes the form

$$T(0,t)=P_0+\sum_{n=1,2,\ldots}^{\infty}B_ne^{i(n\omega_1t-\varepsilon_n)}, \tag{8}$$

with real part

$$T(0,t)=P_0+\sum_{n=1,2,\ldots}^{\infty}B_n\cos(n\omega_1t-\varepsilon_n). \tag{9}$$

The temperature measured at the first thermocouple $f(t)$, whose steady-state profile is shown in Fig. 3, is approximated by a triangle waveform. This waveform is comprised of ascents and descents between the temperature extremes T_l and T_h with a period of $2\pi/\omega_1\approx 200$ s (driving frequency is 5 mHz). Our linear approximations are shown superposed on the temperature profile in the shaded region of Fig. 3.

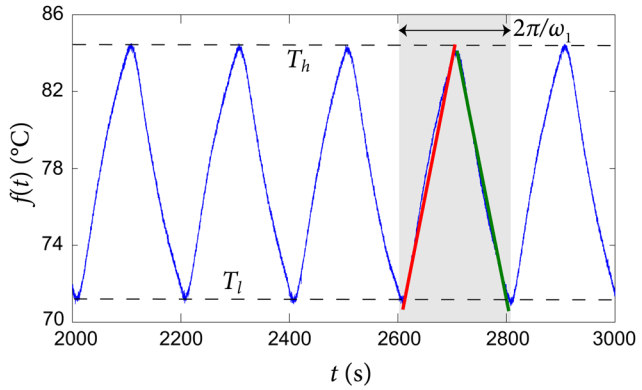

Fig. 3. The temporal variation of the temperature registered by the thermocouple located closest to the heat source (at $x=0$). The shaded region (of period $2\pi/\omega_1$) shows linear fits on the two alternating segments of the waveform.

Next, we write down the Fourier series for a triangle wave of period $2\pi/\omega_1$ oscillating between temperatures T_l and T_h:

$$f(t)=\left(\frac{T_h+T_l}{2}\right)-\frac{2(T_h-T_l)}{\pi^2}\sum_{n=\pm1,\pm3,\ldots}^{\infty}\frac{1}{n^2}e^{in\omega_1t} \tag{10}$$

$$=\langle T(0)\rangle-\frac{4\Delta T}{\pi^2}\sum_{n=1,3,\ldots}^{\infty}\frac{1}{n^2}\cos(n\omega_1t), \tag{11}$$

where $\langle\cdots\rangle$ represents a time average and $\Delta T=T_h-T_l$ is the difference between temperature extremes at $x=0$. Comparing Eqs. (9) and (11), we see that $P_0=\langle T(0)\rangle$ is the mean temperature of the first thermocouple, $\varepsilon_n=0$, and $B_n=-4\Delta T/(\pi^2n^2)$ for odd n while $B_n=0$ for even n. Since the variation of the dc component of the field is linear in space, P_1 can be determined from the average temperature at some other thermocouple. Hence, the solution for our experiment is

$$T(x,t)=P_1x+\langle T(0)\rangle - \frac{4\Delta T}{\pi^2}\sum_{n=1,3,5,\ldots}^{\infty}\frac{1}{n^2}e^{-x/d_n}\cos\left(n\omega_1t-\frac{x}{d_n}\right), \tag{12}$$

where $d_n=\sqrt{2D/\omega_n}$ are "damping lengths" and $P_1=(\langle T(\Delta x)\rangle-\langle T(0)\rangle)/\Delta x$ is the gradient of the average temperatures.

The oscillatory component of the above solution is a periodic function comprising the pulsing frequency ω_1 and (only) its odd multiples ($\omega_3=3\omega_1$, $\omega_5=5\omega_1$, $\omega_7=7\omega_1$, etc.). Armed with Eq. (12), the Fourier composition of the thermal fluctuations shown in Fig. 2 is now quite clear. The disturbance is a sum of spatially damped odd harmonics where the damping of the n'th harmonic is represented by the exponential term $\exp(-x/d_n)$. The damping lengths $d_n=\sqrt{2D/\omega_n}$ are mathematically similar to the skin depth and represent the distance over which the amplitude of each harmonic decreases to $1/e$ of its value at $x=0$. As $d_n\propto 1/\sqrt{n}$ the higher harmonics damp away at smaller distances; ultimately, only the fundamental frequency will survive far

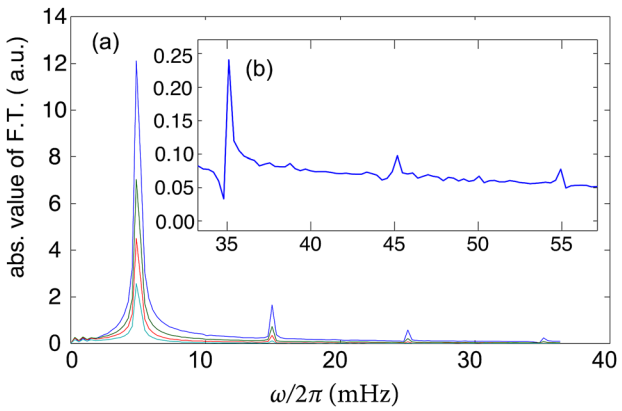

Fig. 4. (a) Fourier transforms of the temperatures measured by the thermocouples. Within a group of peaks, the thermocouples closer to the heat source have the larger components. (b) Close-up of the data from the first thermocouple in the higher frequency range.

from the heat source. In some sense the material is acting like the thermal analogue of a low pass filter.

Figure 4 shows the absolute value of the FFT spectrum of the dynamic equilibrium portion of the temperature data shown in Fig. 2. Prior to taking the FFT we subtracted the mean value; otherwise a large peak at zero frequency dominates the spectrum with its large tails masking out the higher harmonic content. The inset in Fig. 4 vividly shows the presence of discernible harmonics up to 11th order before the peaks sink within the noise limit. (The eleventh order harmonic corresponds to $\omega_{11}/2\pi = 11\omega_1/2\pi = 55$ mHz.)

From the spectral density curves shown in Fig. 4, we can calculate the spectral power under the various frequency peaks (the areas under the peaks), and by comparing these for different thermocouple locations we can determine d_n and subsequently the thermal diffusivity. Figure 5 shows the distance-wise variation of the spectral power for the frequencies ω_1, ω_3, ω_5, and ω_7 on a semi-logarithmic scale. The

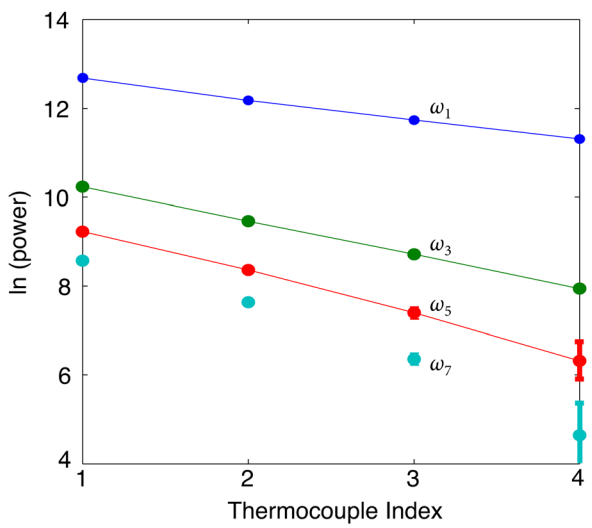

Fig. 5. The logarithm of the area under the peaks (power) in the Fourier transform versus the thermocouple position used as a measure of distance from the heating source. The least square curve fits for the frequencies ω, ω_3, and ω_5 are shown. The slopes of the best-fit lines are used in computing the thermal diffusivity. For most data points, the error bars are smaller than the drawn circles.

horizontal axis is distance, which for convenience is demarcated in terms of the four thermocouples that are separated by 3.3 cm, while the spectral powers are shown along the vertical axis. The slope of the n'th harmonic line is seen from the damping term $\exp(-x/d_n)$ to be $(-1/d_n)$ and immediately determines the damping length of the various harmonics. For the lowest three frequencies, the estimated diffusivities at the 95% coverage probability[12] are (0.81 ± 0.20), (0.88 ± 0.22), and $(0.91 \pm 0.22) \times 10^{-4}$ m^2/s. The accepted value of copper's diffusivity is 1.02×10^{-4} m^2/s showing that our best estimates are reasonably close to the accepted values.

D. Temperature at x = 0

In this section, we take a closer look at the waveform measured by the thermocouple nearest the heat source [shown in Fig. 3 and modeled by Eq. (11)]. The heat flux from the heater is expected to be a square pulse. The temperature, however, will not follow a square pulse. In fact, accurately predicting the temperature variation in an extended solid resulting from a known heating profile is a complicated undertaking and admits analytic expressions only in special cases.[7,11] One tractable scenario is the "lumped capacitance" framework (see p. 51 of Incropera[7]) which uses an energy balance approach to find the transient temperature response of a solid assuming that the entire solid is held at a spatially uniform temperature by virtue of an infinite thermal conductivity. In this simplification, which is reasonably accurate for small objects (more precisely, objects with small Biot numbers), the temperature profile is described by exponential functions and are characterized by a thermal time-constant $\tau = \rho c_v/L$. Here ρ is the material's density, c_v the specific heat capacity, and L the effective length scale over which heat transfer with a source takes place. In short, smaller τ results in rapid variation of the temperature in response to a heat flux, while larger τ shows thermal inertia and sluggish changes in temperature.

In this grossly simplistic lumped model, we can predict the temperature variation at a point extremely close to the heater, say, at its very tip. Suppose the actuation time period is denoted by $\beta = 2\pi/\omega_1$ and the time constant is τ, assumed to be identical for both the ascending and descending segments of the heating cycle. The temperature variation is then approximately given by

$$T_{\text{asc}} = T_l + (T_h - T_l)\,(1 - e^{-t/\tau}), \quad \text{for} \quad t \le \beta/2 \quad \text{and} \tag{13}$$

$$T_{\text{des}} = T_{\text{asc}}(\beta/2)\, e^{-(t-\beta/2)/\tau} \quad \text{for} \quad \beta/2 \le t \le \beta, \tag{14}$$

where T_l and T_h are the temperature extremes. These curves are plotted in Fig. 6(a) for different values of τ/β. A small value of τ/β means smaller inertia relative to longer time periods (lower ω_1); the temperature changes briskly and the exponential rise and fall of the temperature are all more pronounced. The curves are analogous to the charging and discharging of a capacitor. On the other hand, larger values of τ/β imply greater inertia relative to shorter time periods (rapid switching and higher ω_1). The temperature change is slow and does not appreciably change before it switches direction. In this latter case, the profile traverses only a small early segment of the exponential, which enables a piecewise linear approximation to be made. The simulations in Fig.

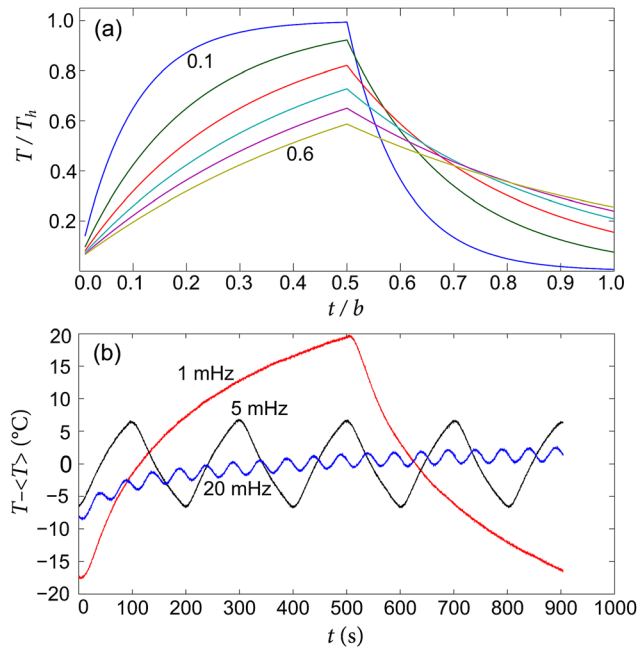

Fig. 6. (a) Simulations showing temperature profile during one switching period for the ratios $\tau/\beta = 0.1$, 0.2, 0.3, 0.4, 0.5, and 0.6 (top to bottom). (b) Temperature deviations from the average measured at the position of the first thermocouple for different actuation frequencies.

6(a) show that this piecewise linear approximation successively becomes more reasonable as τ/β increases.

Now, in the real experiment, we don't measure the temperature at the heater's tip. Instead the nearest thermocouple is ~3 cm from the heater. The temperature waveforms close to the heater and modeled through the above equations will of course alter as the disturbance spreads to the location of the first thermocouple. The primary alteration is through the frequency filtering effect described earlier. So the actual temperature profile $f(t)$ at $x = 0$ depends not only on the profile at the tip of the heater but also the frequency-dependent suppression of the terms. Hence, the waveform $f(t)$ can in principle be controlled by changing the position of the thermocouple, the wattage of the heater or the frequency ω_1. We precisely depict this control in Fig. 6(b). The topmost curve is for a (low) frequency of 1 mHz, which preserves the exponential shape down to the first thermocouple with little damping. On the other extreme is the 20-mHz fluctuation that is not only much smaller in amplitude, but has been rendered into an almost perfect sinusoid with all the higher frequency components effectively damped out. In between these extremes is the fluctuation for 5 mHz, the one used in our experiment and producing a waveform that resembles a triangle waveform. Notice that in a triangular profile, the fractional spectral power in the $n > 1$ harmonics is a mere $\approx 10^{-4}\% = \left(\sum_{n>1}^{\infty} B_n / \sum_{n\geq 1}^{\infty} B_n\right)^2 = (1 - \pi^2/8)^2$, showing that the signal energy in the $n > 1$ harmonics has already been damped quite significantly.

It must also be appreciated that the measurement of the diffusivity is completely independent of the precise waveform observed at the first thermocouple, since the damping length is calculated ratiometrically and the ratio is independent of the coefficients B_n. The temperature profile users obtain in different experimental settings may well be different but this would only change the constants B_n that are not utilized in the determination of the diffusivity.

III. DISCUSSION

We have successfully employed this experiment in our advanced physics laboratory, typically taken by junior students, for four consecutive years. Students need about an hour to familiarize themselves with the hardware, particularly the temperature measurement apparatus and the principle of how the relay circuit works. The data are acquired over a period of about 2 h, and it takes an additional 4–5 h of data manipulation to compute thermal diffusivities and damping lengths.

We believe that this experiment is useful in many respects. From a hardware standpoint, it is relatively straightforward to implement, so modern laboratories equipped with data-acquisition tools can replicate it without difficulty. The mathematical underpinnings are sophisticated and elegant, and so is the instrumentation. The analysis can be framed so that students are required to work out the derivation of the solution, measure the boundary conditions and write down the Fourier series, and understand how the dc component of the oscillations correlate with energy flow. Readers are welcome to consult our laboratory instructions and the associated data acquisition software (LabVIEW program), both of which are available online.[13]

Several important insights can be gleaned from the spatio-temporal temperature data. First, heating and cooling are not instantaneous processes—a square heating pattern does not lead to a square temperature profile; instead, the temperature rises exponentially with a time constant τ. Furthermore, once the heating is turned off, the temperature of the rod follows Newton's Law of Cooling[10] and can be used to estimate the convective heat transfer rates. Second, the experiment directly evokes the original utilization of Fourier's famous series in solving problems in heat diffusion, dating from the early nineteenth century.[14] For our students, observing the Fourier composition of a signal that is outside the domain of electric currents has been inspiring and motivational, particularly when the higher harmonics are naturally filtered as seen here. Third, students gain valuable experience in applying the FFT algorithm while having to keep an eye on frequency re-scaling, sampling rates, resolution in the frequency domain, and the total time for acquisition necessary for a sensible analysis. Needless to say, we like to pose this experiment as a real-world illustration of a beautiful mathematical phenomenon.

ACKNOWLEDGMENTS

The authors would like to thank Suleman Qazi, Umer Hassan, Amrozia Shaheen, and Asma Khalid for performing this experiment and pointing out several improvements. This work was supported by a research grant under the NRPU scheme (No. 2028) of the Higher Education Commission, Pakistan.

[a]Electronic mail: sabieh@lums.edu.pk

[1]A. Bodas, V. Gandía, and E. López-Baeza, "An undergraduate experiment on the propagation of thermal waves," Am. J. Phys. **66**, 528–533 (1998).
[2]M. Berry, "Making light of mathematics," Bull. Am. Math. Soc. (New Series) **40**, 229–237 (2003).
[3]J. A. Scales and R. Snieder, "What is a wave," Nature **401**, 739–740 (1999).
[4]Augstín Salazar, "Energy propagation of thermal waves," Eur. J. Phys. **27**, 1349–1355 (2006).
[5]A. Mandelis, L. Nicolaides, and Y. Chen, "Structure and the reflectionless/refractionless nature of parabolic diffusion-wave fields," Phys. Rev. Lett. **87**, 020801-1—020801-4 (2001).

[6]A. Mandelis, "Diffusion waves and their uses", Phys. Today **66**, 29–34 (2000).
[7]F. P. Incropera, D. P. Dewitt, T. L. Bergmann, and A. S. Lavine, *Fundamentals of Heat and Mass Transfer*, 7th ed. (Wiley, New Jersey, 2012).
[8]J. E. Spuller and R. W. Cobb, "Cooling of a vertical cylinder by natural convection: An undergraduate experiment," Am. J. Phys. **61**, 568–571 (1993).
[9]M. I. Gonzalez and J. H. Lucio, "Investigating convective heat transfer with an iron and a hairdryer," Eur. J. Phys. **29**, 263–273 (2008).
[10]M. S. Anwar and W. Zia, "Curie point, susceptibility, and temperature measurements of rapidly heated ferromagnetic wires," Rev. Sci. Instrum. **81**, 124904–124908 (2010).
[11]H. S. Carslaw and J. C. Jaeger, *Conduction of Heat in Solids*, 2nd ed. (Clarendon Press, Oxford, 1959), pp. 50–92.
[12]L. Kirkup and R. B. Frenkel, *An Introduction to Uncertainty in Measurement* (Cambridge U.P., Cambridge, 2006).
[13]See supplementary material at http://dx.doi.org/10.1119/1.4881608 for our laboratory instructions and the LabVIEW program are available as or at the author-maintained website <http://physlab.lums.edu.pk/index.php/Experiment_in_Lab-II> (see the experiment numbered 2.3).
[14]Fourier's monograph *Théorie analytique de la chaleur* was published in 1822. An original English translation is A. Freeman, *The Analytical Theory of Heat* (Cambridge U.P., Cambridge, 1878).

Water Turbine Demonstration

Most water turbine demonstrations use an enclosed Pelton Wheel and can actually be used for power generation. This little model is purely for demonstration purposes. The disk in the middle has a series of twelve slots. Water from above is forced through these slots, and the resulting jets of water turn the turbine blades. When connected to a water faucet, the device spun rapidly, and, if a belt were connected to the pulley at the top, it could do useful work. It is on long-term loan to the Greenslade Collection from Appalachian State University. (Notes and photograph by Thomas B. Greenslade, Jr., Kenyon College)